

## Electrochemical performance of acicular $\text{Li}_4\text{Ti}_5\text{O}_{12}$ anode material synthesized by ethanol-assisted hydrothermal method

Weiquan Shao<sup>1,2,a,\*</sup>, Shaou Chen<sup>1,2,a,\*</sup>, Lizhu He<sup>1,a</sup>, Hailing Zhu<sup>3,b</sup>, Yueqin Ban<sup>1,a</sup>, Xiaojie Guo<sup>1,a</sup>, Zhen Wang<sup>1,a</sup>, Haifeng Zhao<sup>1,a</sup>, Yingnan Zhang<sup>1,a</sup>

<sup>1</sup> College of physics, Qingdao University, Qingdao 266071, China

<sup>2</sup> Key Laboratory of Photonics Materials and Technology in Universities of Shandong, Qingdao University, Qingdao 266071, China

<sup>3</sup> Department of Physics and Optoelectronic Engineering, Weifang University, Weifang 261061, China.

<sup>a</sup>email: qduswq@163.com, <sup>b</sup>email: zhuzhuhailing@163.com

**Keywords:**  $\text{Li}_4\text{Ti}_5\text{O}_{12}$ ; ethanol-assisted; acicular particle; lithium ion batteries.

**Abstract.** Spinel  $\text{Li}_4\text{Ti}_5\text{O}_{12}$  material were prepared by ethanol-assisted hydrothermal method and sintered at different temperatures. It was found that all of the samples had cubic spinel structure without undesired impurities and the samples showed different morphology as the change of sintering temperature. The sample sintered 750°C delivered a higher discharge capacity than the 700 and 800°C - sample at all the tested C rates. At 10C charge - discharge rate, the obtained discharge capacity of the  $\text{Li}_4\text{Ti}_5\text{O}_{12}$  electrode sintered at 700 and 750°C was about 45.7% and 63.7%, compared to that of a 0.1C rate, while the  $\text{Li}_4\text{Ti}_5\text{O}_{12}$  electrode sintered at 800°C showed capacity retention of only 28.7% at the same C rate, which could be attributed the higher lithium diffusion coefficient and the lower impedance due to the shortened diffusion distance of lithium ions because of the shortening acicular particle.

### Introduction

Lithium ion batteries (LIBs) have become one of the most promising power sources for hybrid electric vehicles (HEVs) and even electric vehicles (EVs) due to the excellent safety features, high energy density and good design flexibility. Thus, the search for electrode materials with high power density, long cycle life, and good safety features has become a key issue over the past several years. Spinel  $\text{Li}_4\text{Ti}_5\text{O}_{12}$  has recently become one of the most important anode materials for lithium-ion batteries, because of its superior capacity retention, thermal stability, nontoxicity, and safety feature [1-3]. However, its large-scale application was restricted by the low electronic conductivity. In order to improve the electronic conductivity, various ways were carried out [4-6]. Thereinto, particle size and morphology controlling were proved to be effective methods [7-9]. In this paper, we report an ethanol-assisted hydrothermal method to synthesize  $\text{Li}_4\text{Ti}_5\text{O}_{12}$  and sintered at different temperatures. It was found that the acicular particle appeared at the sintering temperature of 700°C and 750°C. Thereinto, the sample sintered at 750 °C showed the best electrochemical performance.

### Experimental work

#### Material synthesis

Tetrabutyl titanate ( $\text{Ti}(\text{OC}_4\text{H}_9)_4$ ) and lithium hydroxide monohydrate ( $\text{LiOH}\cdot\text{H}_2\text{O}$ ) were used as starting materials, produced by shanghai aibi Chemistry preparation factory co ltd. In a typical synthesis, 17.02g tetrabutyl titanate was dispersed in 17mL ethyl alcohol forming pale yellow solution. After that, the 20.5mL of 2mol L-1  $\text{LiOH}\cdot\text{H}_2\text{O}$  solution was dropwise added into it to form a white suspension with strong stirring for 15minutes and then transferred to a 100 mL stainless-steel autoclave, which was maintained at 180 °C for 12 h. The white precipitation at the bottom of the

reactor was filtered, washed with ethyl alcohol thoroughly, and then dried in an oven at 80 °C for 6h. Finally, the as-prepared sample was calcined in a muffle by two-step calcinations (first step: 400 °C for 3h, second step: 700, 750, 800 °C for 10h) to form the Li<sub>4</sub>Ti<sub>5</sub>O<sub>12</sub>.

### Materials characterization.

Powder X-ray diffraction (XRD) was carried out using a Rigaku D/max-rB with Cu K $\alpha$ 1 radiation. The diffraction data were obtained at 20=10–80° with scanning rate of 0.01deg·s<sup>-1</sup>. The morphologies of the samples were characterized using a JEOL JSM-6390LV field emission scanning electron microscope (FESEM)

### Electrode preparation and electrochemical characterization

Electrochemical measurements were measured with CR2032 coin cells in which a lithium metal foil was used as the counter and reference electrode. Working electrode was prepared by a slurry coating procedure. The slurry consisted of 80 wt% active materials, 10 wt% acetylene black, 10 wt% polyvinylidene fluoride (PVDF) binder, and was uniformly coated onto a copper foil. Then the electrode was dried in vacuum at 120 °C for 10 h before battery assembling. A solution of 1 mol LiPF<sub>6</sub> dissolved in a mixture of ethylene carbonate (EC) and diethyl carbonate (DEC) (V:V = 1:1) was used as the electrolyte, and the Celgard 2400 membrane was used as the separator. The coin cells were assembled in an argon-filled glove box, in which the concentration of water and oxygen was kept below 0.1 ppm. Room temperature galvanostatic charge/discharge tests were performed between 1.0 and 2.5 V at different current densities on a CT2001A cell test instrument (LANHE Electronic Co.). The AC impedance spectra of the samples were performed between 0.01Hz and 10000Hz on a Electrochemical workstation (CHI600E, Shanghai Chenhua Instrument Co.)

## Results and discussion

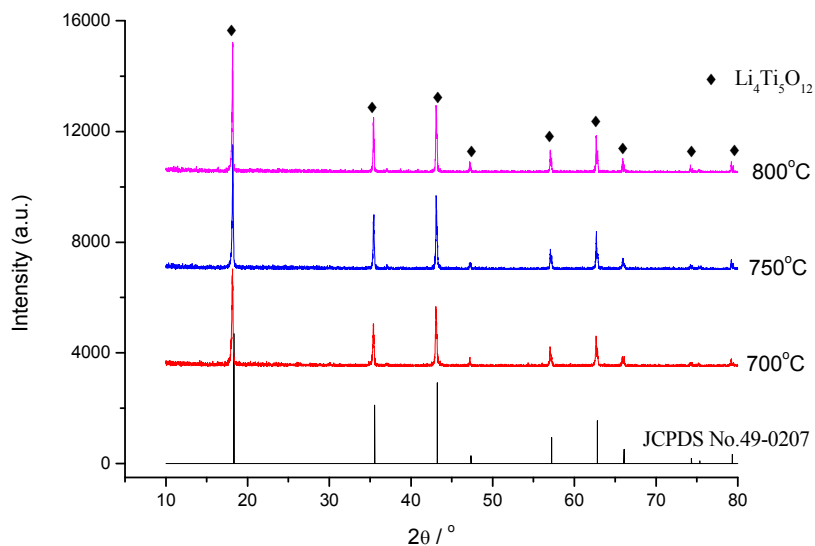


Fig. 1 X-ray diffraction patterns of samples prepared at different sintering temperatures

Fig.1 showed the XRD patterns of the samples prepared by the hydrothermal method and sintered at 700, 750, 800°C. The hydrothermal process does not lead to a spinel structure but an intermediate phase with a layered titanate structure and a chemical formula of the orthorhombic Li<sub>1.81</sub>H<sub>0.19</sub>Ti<sub>2</sub>O<sub>5</sub>·nH<sub>2</sub>O [10]. The samples all presented well-defined peaks at 2θ of 18.3°, 35.6°, 43.2°, 47.3°, 57.2°, 62.8° and 66.1°, which were assigned to the (111), (311), (400), (331), (333), (440) and (531) planes of crystalized Li<sub>4</sub>Ti<sub>5</sub>O<sub>12</sub> respectively (JCPDS No.49-0207) [11].

Fig. 2 showed the plane-view SEM images of samples prepared at different sintering temperatures. After calcining at 700 °C, pure crystalline phase of acicular spinel Li<sub>4</sub>Ti<sub>5</sub>O<sub>12</sub> was obtained. As the temperature increasing to 750 °C, the acicular particle became shortening gradually. When the sintering temperature was 800 °C, the acicular particle disappeared completely. The

acicular structure could effectively shorten the Li-ion diffusion path, which was helpful for the electronic conductivity improvement. Moreover, the particle aggregation appeared as the sintering temperature increasing, which would influence the contact area between the active materials and the electrolyte.

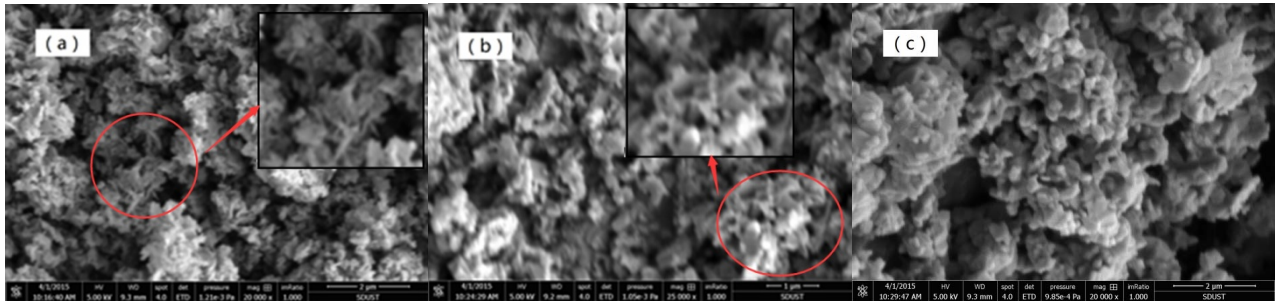


Fig.2 SEM images of samples sintered at 700 °C(a), 750 °C(b) , 800 °C (c)

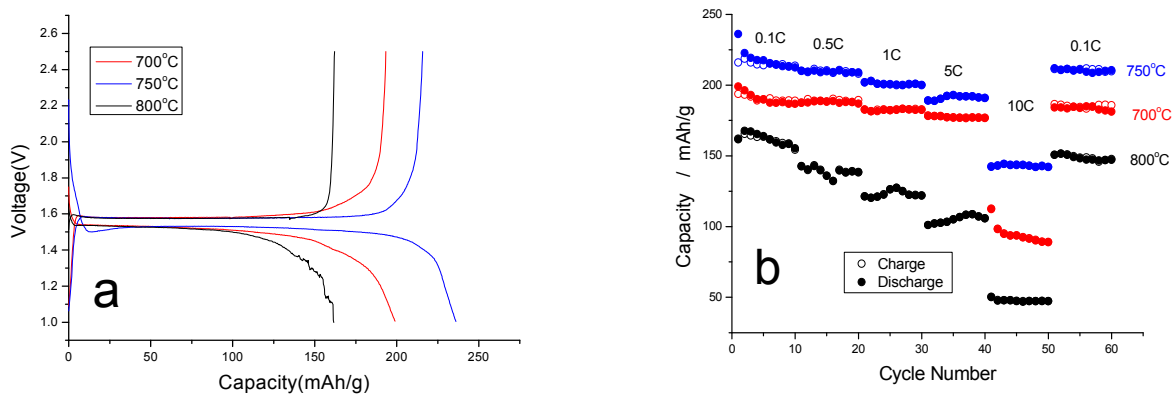


Fig. 3 Voltage profiles (a) and Cycling performance (b) for samples prepared at different sintering temperatures

Fig.3(a) showed the initial charge and discharge curves at 0.1C for  $\text{Li}_4\text{Ti}_5\text{O}_{12}$  samples sintered at different temperatures. All samples showed flat plateaus around 1.5 V (vs  $\text{Li}/\text{Li}^+$ ), which corresponded to the reversible phase transition between  $\text{Li}_4\text{Ti}_5\text{O}_{12}$  and  $\text{Li}_7\text{Ti}_5\text{O}_{12}$  [12]. The first discharge capacity of the  $\text{Li}_4\text{Ti}_5\text{O}_{12}$  electrode sintered at 750 °C was somewhat higher than that of the sample sintered at 700 °C and 800 °C.

Fig.3(b) showed the rate performance of the  $\text{Li}_4\text{Ti}_5\text{O}_{12}$  electrodes sintered at different temperatures. Clearly, the sample sintered 750 °C delivered a higher discharge capacity than the 700 and 800 °C- sample at all the tested C rates. At 10C charge–discharge rate, the obtained discharge capacity of the  $\text{Li}_4\text{Ti}_5\text{O}_{12}$  electrode sintered at 700 and 750 °C was about 45.7% and 63.7%, compared to that of a 0.1C rate, while the  $\text{Li}_4\text{Ti}_5\text{O}_{12}$  electrode sintered at 800 °C showed capacity retention of only 28.7% at the same C rate. Moreover, the capacity changed a little at 0.1C rate for all the samples after 50 cycling at different C rates, which indicated the stable structure for  $\text{Li}_4\text{Ti}_5\text{O}_{12}$  anode materials. Compared to that of the sample sintered at 800 °C, the better electrochemical performances for 700 and 750 °C-sample could be attributed to the acicular structure and the less particle aggregation, which would influence the contact area between the active materials and the electrolyte and further decreasing the irreversible capacity loss caused by the concentration polarization when the current density was enhanced [13].

Fig. 4(a) showed the results of AC impedance spectra of the  $\text{Li}_4\text{Ti}_5\text{O}_{12}$  electrodes. The impedance spectra were composed of one semicircle at higher frequencies followed by linear part at lower frequencies. AC impedance spectra are fitted by Z-View from Sai software set using an equivalent circuit (shown in the inset of Fig.4(a)). In the equivalent circuit,  $R_s$  and  $R_{ct}$  were the solution

resistance and charge transfer resistance, respectively. CPE was placed to represent the double layer capacitance and passivation film capacitance. W is the Warburg impedance caused by a semi-infinite diffusion of  $\text{Li}^+$  in the electrode. The parameters of the equivalent circuit were recorded in Table 1. It could be found that the sample sintered at 750 °C had the lower resistance, which indicated the best electrochemical performance for the sample.

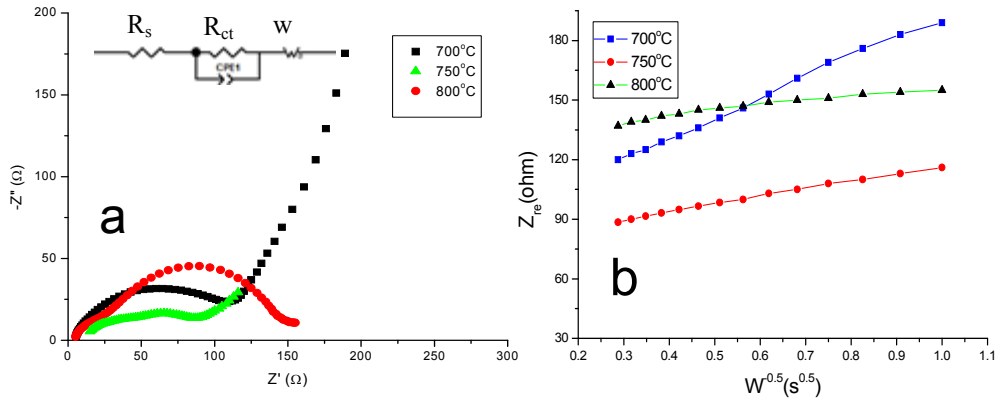


Fig. 4 (a) The impedance spectra and (b) the relationship between real impedance and low frequencies of the samples prepared at different sintering temperatures

Table.1 The parameters obtained from the electrochemical impedance.

Sample	$R_s/\Omega$	Error of $R_s/\%$	$R_{ct}/\Omega$	Error of $R_{ct}/\%$	$\sigma_\omega/\Omega \text{ cm}^2 \text{s}^{-0.5}$	$D/\text{cm}^2 \text{s}^{-1}$
700°C	3.77	3.43	95.87	0.919	102.2	$1.58 \times 10^{-9}$
750°C	3.94	11.41	52.8	1.82	78.33	$2.68 \times 10^{-9}$
800°C	4.64	4.28	141.5	3.74	132.2	$9.39 \times 10^{-10}$

The relationship between the real impedance and the low frequencies was illustrated in Fig. 4(b). The relation was governed by Eq.(1). The diffusion coefficient of the lithium ions in the bulk electrode materials was calculated by Eq.(2)[14].

$$Z_{re} = R_s + R_{ct} + \sigma \omega^{-1/2} \quad (1)$$

$$D = \frac{R^2 T^3}{2 A^2 F^4 C^2 \sigma^2} \quad (2)$$

where  $\sigma$ : Warburg impedance coefficient,  $\omega$ : angular frequency in the low frequency region,  $D$ : diffusion coefficient,  $R$ : the gas constant,  $T$ : the absolute temperature,  $F$ : Faraday's constant,  $A$ : the area of the electrode, and  $C$ : molar concentration of  $\text{Li}^+$  ions. From Table 1, it could be found that the sample sintered at 750 °C had larger  $\text{Li}^+$  diffusion coefficient than others due to the shortened diffusion distance of lithium ions because of the shortening acicular particle, which confirmed that the appropriate sintering temperature was beneficial to the rate capability and reversible intercalation and de-intercalation of  $\text{Li}^+$ .

## Conclusion

Spinel  $\text{Li}_4\text{Ti}_5\text{O}_{12}$  material were prepared by ethanol-assisted hydrothermal method and sintered at different temperatures. On the basis of the electrochemical properties at 10C, the capacity for samples sintered at 700 °C, 750 °C and 800°C was 89.4mAh/g, 141.4 mAh/g and 47.6mAh/g, respectively. The diffusion coefficient of the sample was  $2.68 \times 10^{-9} \text{ cm}^2 \text{s}^{-1}$ (750 °C),  $1.58 \times 10^{-9} \text{ cm}^2 \text{s}^{-1}$ (700 °C),  $9.39 \times 10^{-10} \text{ cm}^2 \text{s}^{-1}$ (800°C), respectively. The sample sintered at 750 °C showed much better C-rate performance at 0.1-10C rate than the samples sintered at 700 °C and 800°C, which could be attributed

the higher lithium diffusion coefficient and the lower impedance due to the acicular particle shortening.

### Acknowledgement

This work was supported by the Natural Science Foundation of Shandong Province (ZR2014EMQ005, ZR2010EQ001), the Project of Shandong Province Higher Educational Science and Technology Program (Grant No. J14LJ08, J15LA13), the Taishan Scholars Program of Shandong Province (ts20120528), China.

### References

- [1] M. Kitta, T. Akita, S. Tanaka, M. Kohyama. Characterization of two phase distribution in electrochemically-lithiated spinel  $\text{Li}_4\text{Ti}_5\text{O}_{12}$  secondary particles by electron energy-loss spectroscopy, *J. Power Sources*. 237(2013)26 -32.
- [2] Takeuchi T, Kageyama H, Nakanishi K, et al. Application of graphite-selid electrolyte composite anode in all-solid-state lithium secondary battery with  $\text{Li}_2\text{S}$  positive electrode, *Solid State Ionics*. 262(2014)138-142.
- [3] Mc Sweeney W, Lotty O, Glynn C, et al. The influence of carrier density and doping type on lithium insertion and extraction processes at silicon surfaces, *Electrochimica Acta*. 135(2014)356-367.
- [4] Chih-Yuan Lin, Yi-Ruei Jhan, Jenq-Gong Duh. Improved capacity and rate capability of Ru-doped and carbon-coated  $\text{Li}_4\text{Ti}_5\text{O}_{12}$  anode material, *Journal of Alloys and Compounds*. 509(2011)6965-6968.
- [5] Abdelfattah Mahmouda, José Manuel Amarilla , Ismael Saadoune, et al. Effect of thermal treatment used in the sol-gel synthesis of  $\text{Li}_4\text{Ti}_5\text{O}_{12}$  spinel on its electrochemical properties as anode for lithium ion batteries, *Electrochimica Acta*. 36(2015)213-222.
- [6] Wei Fang, Xinqun Cheng, PengJian Zuo, et al. Hydrothermal-assisted sol-gel synthesis of  $\text{Li}_4\text{Ti}_5\text{O}_{12}/\text{C}$  nano-composite for high-energy lithium-ion batteries, *Solid State Ionics*, 244(2013)52-56.
- [7] Chert W N, Jiang H, Hu Y J, et al. Mesoporous single crystals  $\text{Li}_4\text{Ti}_5\text{O}_{12}$  grown on GO as high rate anode materials for lithium-ion batteries , *Chemical Communications*. 50(2014)8856-8859.
- [8] Meijuan Hu, Yinzhu Jiang, Mi Yan. High rate  $\text{Li}_4\text{Ti}_5\text{O}_{12}-\text{Fe}_2\text{O}_3$  and  $\text{Li}_4\text{Ti}_5\text{O}_{12}-\text{CuO}$  composite anodes for advanced lithium ion batteries, *Journal of Alloys and Compounds*. 603(2014)202-206.
- [9] Liping Wang, Haiquan Zhang, Qijiu Deng. Superior rate performance of  $\text{Li}_4\text{Ti}_5\text{O}_{12}/\text{TiO}_2/\text{C/CNTs}$  composites via microemulsion-assisted method as anodes for lithium ion battery, *Electrochemical Acta*. 142(2014)202-207.
- [10] Y. Tanaka, M. Tsuji, M. Abe. Selective adsorption of dimethylarsinic acid by Synthetic inorganic ion exchangers, *Chem Lett*. 17(1990) 661-667.
- [11] Tang Y F, Huang F Q, Zhao W, Liu Z Q, Wan D Y. Synthesis of graphene-supported  $\text{Li}_4\text{Ti}_5\text{O}_{12}$  nanosheets for high rate battery application, *Journal of Materials Chemistry*. 22(2012)11257-11260.
- [12] T.-F. Yi, Y. Xie, Q. Wu, H. Liu, L. Jiang, M. Ye, R. Zhu. High rate cycling performance of lanthanum-modified  $\text{Li}_4\text{Ti}_5\text{O}_{12}$  anode materials for lithium-ion batteries, *J. Power Sources*. 214(2012) 220-226.
- [13] H.B. Lin, Y.M. Zhang, J.N. Hu.  $\text{LiNi}_{0.5}\text{Mn}_{1.5}\text{O}_4$  nanoparticles: Synthesis with synergistic effect of polyvinylpyrrolidone and ethylene glycol and performance as cathode of lithium ion battery, *Journal of Power Sources*. 257(2014)37-44.
- [14] Chun-Kai Lan, Shang-I. Chuang, Qi Bao, Yen-Ting Liao, Jenq-Gong Duh. One-step argon/nitrogen binary plasma jet irradiation of  $\text{Li}_4\text{Ti}_5\text{O}_{12}$  for stable high-rate lithium ion battery anodes. *Journal of Power Sources*, *Journal of Power Sources*. 257(2015) 660-667.